REPORT DOCUMENTATION PAGE

Form Approved
OMB No. 0704-0188

1. AGENCY USE ONLY *(Leave blank)*

2. REPORT DATE
May 1992

3. REPORT TYPE AND DATES COVERED
Technical Paper

4. TITLE AND SUBTITLE
MIRACAL: A Mission Radiation Calculation Program for Analysis of Lunar and Interplanetary Missions

5. FUNDING NUMBERS
WU 593-42-31-01

6. AUTHOR(S)
John E. Nealy , Scott A. Striepe, and Lisa C. Simonsen

7. PERFORMING ORGANIZATION NAME(S) AND ADDRESS(ES)
NASA Langley Research Center
Hampton, VA 23665-5225

8. PERFORMING ORGANIZATION REPORT NUMBER
L-17044

9. SPONSORING/MONITORING AGENCY NAME(S) AND ADDRESS(ES)
National Aeronautics and Space Administration
Washington, DC 20546-0001

10. SPONSORING/MONITORING AGENCY REPORT NUMBER
NASA TP-3211

11. SUPPLEMENTARY NOTES

12a. DISTRIBUTION/AVAILABILITY STATEMENT
Unclassified–Unlimited

Subject Category 93

12b. DISTRIBUTION CODE

13. ABSTRACT *(Maximum 200 words)*
A computational procedure and data base are developed for manned space exploration missions for which estimates are made for the energetic particle fluences encountered and the resulting dose equivalent incurred. The data base includes the following options: statistical or continuum model for ordinary solar proton events, selection of up to six observed large proton flare spectra, and galactic cosmic ray fluxes for elemental nuclei of charge numbers 1 through 92. The program requires as input trajectory definition information and specification of optional parameters, which include desired spectral data and nominal shield thickness. The procedure may be implemented as an independent program or as a subroutine in trajectory codes. This code should be most useful in mission optimization and selection studies for which radiation exposure is of special importance.

14. SUBJECT TERMS
Computational radiation data base; Deep-space exploration

15. NUMBER OF PAGES
15

16. PRICE CODE
A03

17. SECURITY CLASSIFICATION OF REPORT
Unclassified

18. SECURITY CLASSIFICATION OF THIS PAGE
Unclassified

19. SECURITY CLASSIFICATION OF ABSTRACT

20. LIMITATION OF ABSTRACT

Abstract

A computational procedure and data base are developed for manned space exploration missions for which estimates are made for the energetic particle fluences encountered and the resulting dose equivalent incurred. The data base includes the following options: statistical or continuum model for ordinary solar proton events, selection of up to six observed large proton flare spectra, and galactic cosmic ray fluxes for elemental nuclei of charge numbers 1 through 92. The program requires as input trajectory definition information and specification of optional parameters, which include desired spectral data and nominal shield thickness. The procedure may be implemented as an independent program or as a subroutine in trajectory codes. This code should be most useful in mission optimization and selection studies for which radiation exposure is of special importance.

Introduction

When man ventures into interplanetary space, the ionizing radiation environment and the resulting exposure will be orders of magnitude greater than that which exists on Earth. This aspect of space travel is described in detail in reference 1. The most hazardous radiation in deep space consists of energetic protons emitted by the Sun during large proton flares, and galactic cosmic rays (GCR) composed of stripped nuclei of the atomic elements. The Earth is shielded from these particles to a great extent by both the atmosphere and the intrinsic magnetic field, which deflects and/or traps charged particles. Thus, astronauts in low Earth orbit (beneath the trapped particle regions) are substantially protected from solar and galactic charged particles. However, for lunar and interplanetary missions, a space transportation vehicle and its occupants are subject to the effects of the essentially unattenuated deep-space environment, and substantial shielding may be required to ensure the safety and well-being of crew members.

The interplanetary radiation environment can vary both temporally and spatially by many orders of magnitude. Thus, the radiation doses incurred can vary considerably, depending on factors such as mission duration, trajectories chosen for transit, the time at which the mission takes place during a solar cycle, and the extent of shielding provided. The tremendous advances in man's knowledge of the deep-space environment, provided by measurements from instrumented satellite platforms, allow the construction of a data base that can reasonably represent the magnitudes and variabilities of both the solar protons and the GCR fluxes. In addition, recent enhancements in predicting the phenomena associated with high-energy charged particle transport through shield media (refs. 2 and 3) allow the extension of the environmental data base to include estimates of corresponding incurred doses for various shield thicknesses. A comprehensive and detailed description of transport computational methods for charged particle space radiation may be found in reference 4. The present work attempts to utilize this methodology in order to define and establish a data base that may be readily applied to various interplanetary mission scenarios. An algorithm is developed that uses this data base in conjunction with pertinent mission definition parameters (such as trajectory specification, proximity to the Sun and planets, shielding provided, and time spent in planetary orbit or on the surface) to provide estimates of cumulative particle fluences (time-integrated fluxes) and incurred dose as a function of mission elapsed time. The following sections describe the structure and contents of the current data base, computational options included in the algorithm, and sample results.

Symbols and Abbreviations

BFO	blood-forming organ
BRYNTRN	baryon transport computer code
CAM	Computerized Anatomical Man
CREME	Cosmic Ray Effects on Microelectronics
F_{sh}	shadow factor
GCR	galactic cosmic rays
H	dose equivalent
MIRACAL	Mission Radiation Calculation program
NCRP	National Council on Radiation Protection and Measurement
R	radial distance from Sun
r	distance from spacecraft to planet center, km
r_b	radius of body that spacecraft is orbiting, km
t	thickness, g/cm^2
w	weighting factor
Z	atomic number
ϕ_i	differential flux of element i, particles/(cm^2-sec-MeV)

Radiation Environment and Exposure Model

General Description

The data base consists of three basic sections: (1) environmental fluence data, (2) the corresponding slab dose equivalent results for various water shield thicknesses, and (3) detailed dose equivalent calculations using the Computerized Anatomical Man (CAM) model. The interplanetary ionizing radiation environment is represented in the present model by the nuclei of the chemical elements of charge number Z, from 1 (protons), 2 (alphas), 3 (lithium), ..., up to and including 92 (uranium). Numerous measurements and analyses indicate that these particles are responsible for practically all the energy deposition in condensed matter in interplanetary space. The modeled environment consists of galactic cosmic ray data, large proton flare data, and ordinary proton flare data. The temporal and spatial variations of each of these constituents are also accounted for where appropriate. For the GCR environment, the model uses the CREME code (ref. 5), which specifies a solar cycle duration of 10.908 years, calculable from epoch A.D. 1975.144 as the reference solar minimum. Solar flare proton fluxes as observed at Earth are assumed to vary spatially within the solar system as $1/R^2$ (ref. 6), where R is the distance of the target (spacecraft) from the Sun in astronomical units (AU).

The fluences and doses incurred from passage through the Van Allen belts are not addressed in the data base. For a moderately shielded spacecraft, the doses incurred during single transits through the trapped belts are not significant compared with the long-term free-space contributions from GCR and solar proton events (ref. 7). However, cumulative doses may be significant for multiple-pass trajectories spiraling through the trapped regions (for example, during low-thrust escapes or captures at Earth).

The dose equivalents corresponding to the GCR and flare fluences are included in the data base by using computational results obtained from earlier transport calculations. The transport calculations were performed with two deterministic nucleon and heavy-ion transport computer codes to predict the propagation and interactions of the free-space nucleons and heavy ions through various media. For large solar flare radiation, the baryon transport code BRYNTRN was used (ref. 2). For galactic cosmic rays, an existing heavy-ion transport code was integrated with the BRYNTRN code to include the transport of high-energy heavy ions up to atomic number 28 (ref. 3). The dose equivalents were evaluated according to the quality factors specified by the International Commission on Radiological Protection (ref. 8). Dose equivalent values in the data base are expressed in SI units of centisieverts, which are numerically equal to the commonly used rem units.

The attenuating medium is considered to be water (H_2O) for the external shield and human tissue. Even though water may be somewhat impractical as an external shield material because of structural considerations, transport calculations have indicated that other low-density, high-hydrogen-content materials such as polyethylene or lithium hydride behave in a manner similar to H_2O in their heavy-ion attenuation characteristics, and such materials are considerably more efficient heavy-ion shields than high-atomic-number substances. Water also provides a good simulation of human tissue and of food stuffs or waste products, which may be present in large quantities on exploratory class missions. The dose calculations for water can provide good estimates for equivalent thicknesses of materials other than water by incorporating previously calculated buildup factors if such data are available. Buildup factor methods essentially relate thicknesses of different materials for which equal doses are obtained for given environment spectra (see, for example, ref. 9). Thus, reasonable shield effectiveness estimates may be made for candidate low-density shield media by considering a single material, which of course also greatly simplifies and reduces the size of the data base.

No limits on radiation exposure have been established for exploration class missions, such as Mars missions. The radiation exposure guidelines for space missions have undergone several revisions, and studies continue to be made that strive to better define human risk in terms of exposure. The National Council on Radiation Protection and Measurements (NCRP) has recommended that the radiation limits established for low Earth orbit, as shown in table I, be used as guidelines for such missions. A recent recommendation from the Council (ref. 1) states

> ".....exploratory missions with considerable, and perhaps unknown, risks should receive separate and individual consideration with the constraints given in [table I] serving as guidelines only."

The NCRP guideline limits refer to dose equivalent evaluation for transport within a semi-infinite slab tissue medium. Dose equivalent values for such slab calculations are included in the data base for each of the environment constituents modeled.

Table I. NCRP-98 Dose Equivalent Limit Guidelines

Exposure	Limit, cSv, for—		
	Skin	Eye	BFO
30-day	150	100	25
Annual	300	200	50
Career	600	400	[a]100–400

[a]Age and gender dependent.

In addition to the basic semi-infinite slab calculations, the MIRACAL model also provides dose evaluation by using the detailed body geometry of the Computerized Anatomical Man (CAM) model (ref. 10) for the skin, ocular lens, and blood-forming organs (BFO). This is accomplished by incorporating the appropriate CAM tissue thicknesses, which utilize an evenly spaced distribution of 512 rays over a 4π solid angle for the 50th percentile United States Air Force male. Specific target point locations within the body and corresponding ray diagrams may be found in the CAM model document. The skin and blood-forming organ (BFO) distributions are both average distributions of 33 locations in the human body, while the ocular lens distribution is for only one location. Often, the skin and BFO doses are approximated by slab doses at depths of 0 and 5 cm in tissue, respectively. Characteristically, the more detailed CAM calculation results in 20 to 50 percent lower doses than the corresponding slab approximations, with the degree of reduction dependent on the energetic particle environment spectrum.

Galactic Cosmic Rays (GCR)

GCR flux contributions for this environmental model include nuclei of the first 92 elements. The magnitudes of the fluxes are greatest during solar minimum, or quiet Sun conditions, since the interplanetary magnetic field is weakest in this period and more intergalactic particles gain access to the solar system. Fluxes used in the data base have been obtained from the Naval Research Laboratory CREME (Cosmic Ray Effects on Microelectronics) model (ref. 5) and are illustrated in figure 1 as a function of energy per unit mass for the solar minimum condition. The protons (H, $Z = 1$) are most numerous, and alphas (He, $Z = 2$) are second in abundance. The remaining elements are also shown in figure 1, for convenience of illustration, in three groups: the lighter mass elements (Li–F, $Z = 3$–9), the intermediate mass elements (Ne–Ni, $Z = 10$–28), and the heavier elements (Cu–U, $Z = 29$–92). The data base, however, contains the energy distribution of each individual species. At solar maximum, GCR fluxes are reduced substantially. The amounts of flux reductions for the various species groups are shown in figure 2 in terms of the energy dependent ratios of solar maximum to solar minimum fluxes (ref. 5). The flux reduction is most pronounced for protons, while the particles of higher energies (several GeV and above) are only slightly affected by solar cycle variation.

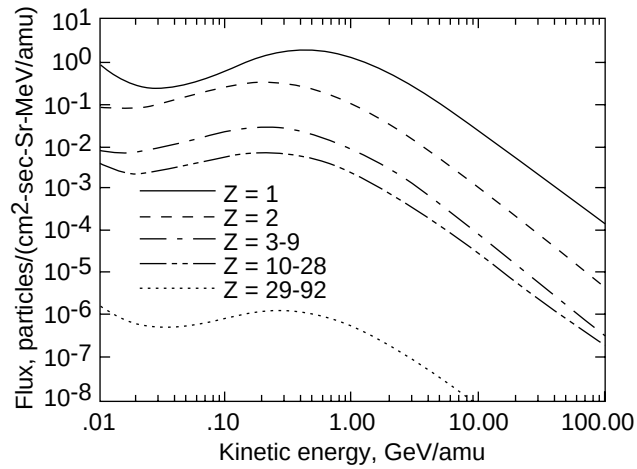

Figure 1. Galactic cosmic ray differential flux spectra at solar minimum for selected elemental groups.

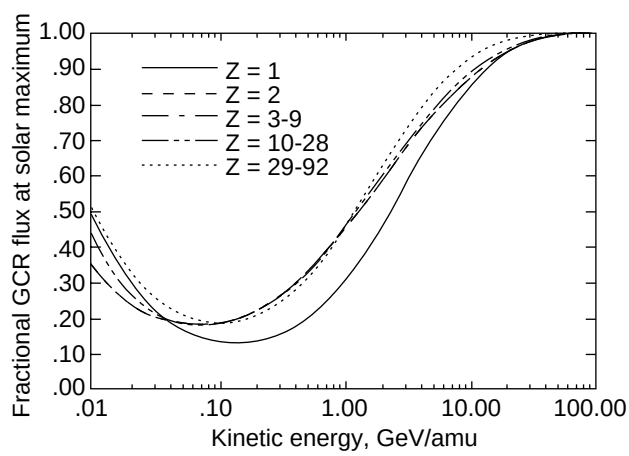

Figure 2. Ratios of galactic cosmic ray differential flux at solar maximum to corresponding flux at solar minimum for selected elemental groups.

The GCR flux variation throughout the approximately 11-year solar cycle is calculated with a weighting (modulation) function that determines the fractional solar minimum and solar maximum fluxes observed at a given time within the cycle. The modulation of the GCR flux depends directly on the intensity of solar activity. Solar activity may be gauged by a variety of observed quantities:

sunspot numbers, various magnetic indices, ground-based neutron monitors, electromagnetic radiation fluxes, etc., any of which can be used as a modulation parameter. The present model uses the intensity of the 10.7-cm microwave flux (F10.7 index) because it seems to be somewhat less sporadic than other indices. The modulation function, shown in figure 3, is derived from the F10.7 index variation during solar cycle 21 (ref. 11). With the highest GCR fluxes occurring near solar minimum, the modulation represents a reduction factor for the peak GCR flux as a function of time throughout the cycle. This weighting function has a reciprocal relationship to the magnitude of the 10.7-cm flux, which characteristically is observed to return to approximately the same level at solar minimum for each solar cycle. However, during solar maxima, levels of solar activity are observed to vary from cycle to cycle. The variation of the GCR flux of species i, ϕ_i, at a given time t is expressed in terms of the modulation function $w(t)$, as

$$\phi_i(t) = w(t)\phi_i^{\text{solar min}} + [1 - w(t)]\phi_i^{\text{solar max}}$$

Since solar cycle 21 was a relatively weak cycle during active Sun years, GCR fluxes in the present model never attain their minimum values. Consequently, some degree of conservatism is present in the modeled GCR fluxes.

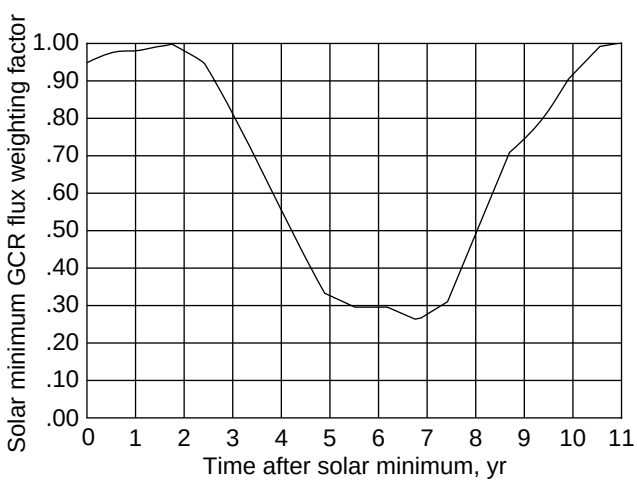

Figure 3. Modulation function for galactic cosmic ray flux as derived for solar cycle 21 in terms of the weighting factor for observed peak (solar minimum) flux.

Transport calculations for the maximum and minimum GCR fluxes have been made for water slab media (ref. 12) with the resultant dose equivalent versus depth functions shown in figure 4. The dose rate for solar minimum conditions is approximately a

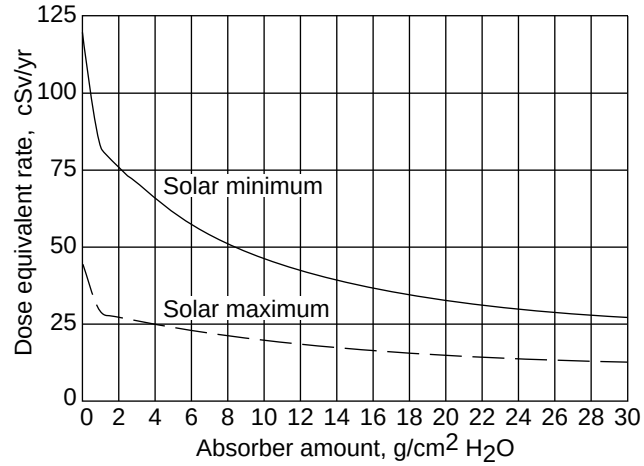

Figure 4. Annual incurred dose equivalent for galactic cosmic rays at solar minimum and solar maximum as a function of water slab thickness.

factor of 2 higher than that for solar maximum. In the model dose calculation, the GCR dose equivalent rate, H_{GCR}, is evaluated with the solar modulation function in a manner similar to the flux:

$$H_{\text{GCR}}(t) = w(t)H_{\text{GCR}}^{\text{solar min}} + [1 - w(t)]H_{\text{GCR}}^{\text{solar max}}$$

The GCR dose equivalents to the skin, ocular lens, and BFO are also estimated by using the CAM model. The tissue thickness distributions for these body components are shown in figure 5, where percent thickness less than a given value is expressed in terms of thickness values at the body target points. These distributions are used in a manner analogous to a cumulative probability distribution function of thicknesses seen in any direction about a given point. Figure 6 shows the GCR dose equivalent variation with external shield amount for the CAM BFO calculations at extremes of the solar cycle. The CAM BFO results may be related to the corresponding 5-cm slab doses by comparing values in figures 4 and 6. For example, the slab dose equivalent for a total thickness of 8 g/cm^2, when taken to represent the 5-cm depth dose with 3 g/cm^2 protection, is 51 cSv/yr. The corresponding 3 g/cm^2 value of figure 6 is 41 cSv/yr, or about 20 percent less than the slab value, indicating the conservative nature of the 5-cm slab dose approximation to the actual BFO dose.

Large Proton Flares

During the 5 to 7 years of relatively high solar activity within a solar cycle, observations show that one or two very large flares may produce more high energy protons than the sum of the 50 or more smaller proton events normally occurring during active Sun conditions. The proton fluences for the six largest

flares observed during the last four solar cycles (19–22) are included in the MIRACAL data base. The integral fluences for these flares are given in figure 7. Except for the near certainty that such events take place during years of solar maximum, these large flares are practically unpredictable with regard to time of occurrence and spectral characteristics. Prior to the latter months of 1989, spectral data for only three of these large flares existed and were used in various radiation exposure analyses (refs. 13 and 14). No large flares in this category occurred in solar cycle 21 (1975–1986); however, in the latter part of 1989, three large events were observed. Their energy spectra and temporal behavior were accurately measured on the NOAA GOES-7 platform (ref. 15).

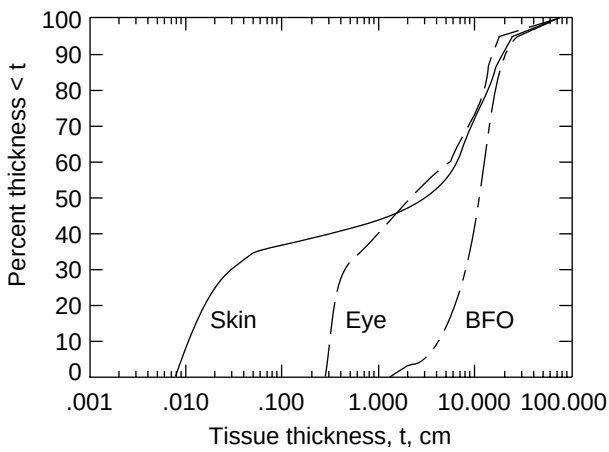

Figure 5. Distribution functions of tissue thickness for skin, ocular lens, and blood-forming organs for the computerized anatomical man (CAM) model.

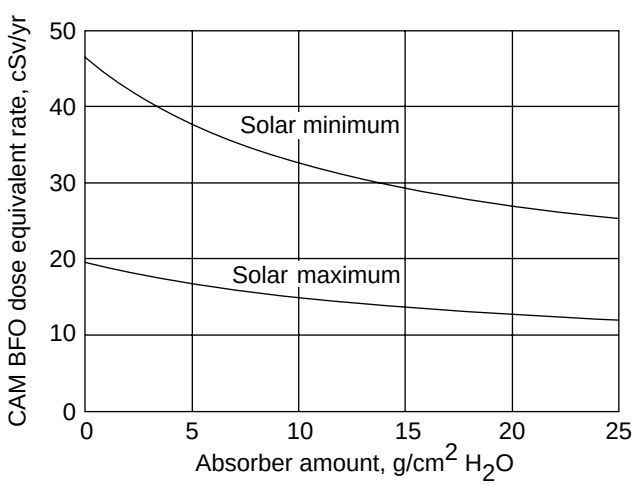

Figure 6. Annual incurred dose equivalent for galactic cosmic rays evaluated with CAM BFO thickness distribution.

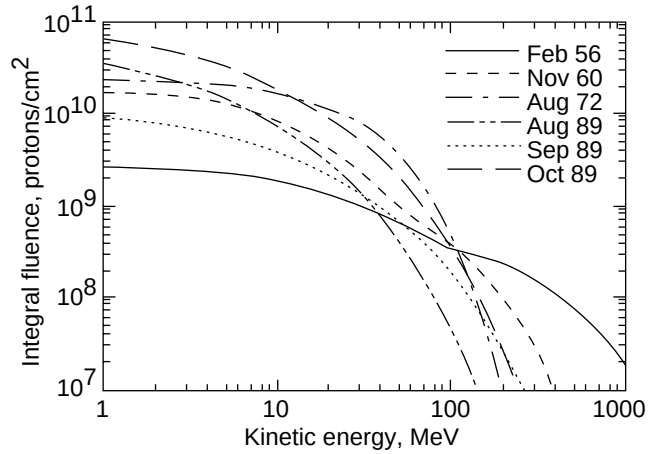

Figure 7. Integral fluence energy spectra for six large solar proton flares.

The rarity of large flare events and the unpredictability of their spectral properties practically preclude a statistical approach for mission analysis applications. Therefore, the present model formulation requires specification of individual large flare spectra and the time of occurrence for each mission calculation. The question of which large flares (if any) to include in the calculation is left to the judgment of the user, who may base his choice on several factors. For example, consideration should be given to mission duration and time of mission within the solar cycle. For missions taking place during solar minimum years, dose contributions from large flares may be reasonably omitted. The combination of the three 1989 flare spectra would be representative of a severe, large flare environment during solar maximum for which spectral characteristics are best known. The 1956 flare spectrum is an isolated case for which high energy proton fluxes were extremely large. Since a best, or most reasonable, large flare environment for a given mission is conjectural, mission analyses with various combinations of flare spectra as parameters may be preferable.

The modeled dose-versus-depth functions for each of the large flares are given in figure 8. As expected, the flares with highest fluxes at low energies, such as the August 1972 and August 1989 events, deliver very large doses for thin shield amounts. For thicker shields (15–20 g/cm^2), the spectra that dominate at higher energies (February 1956 and November 1960) result in greater dose values. The detailed CAM model functions for these flares are also included in the data base. The CAM BFO results shown in figure 9 may be compared with the appropriate slab doses of figure 8 in a manner similar to that described for the GCR. For the flares, the 5-cm slab doses are even more conservative than for the GCR when

compared with the corresponding CAM BFO values. Figures 7, 8, and 9 show the flare fluences, slab dose equivalent, and CAM dose equivalent, respectively, at a distance from the Sun of one astronomical unit (AU).

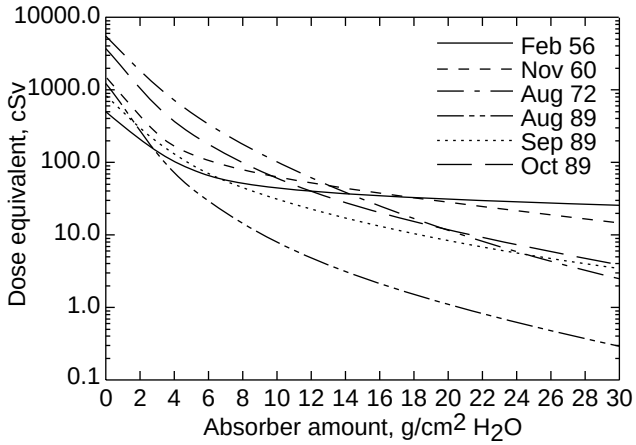

Figure 8. Dose equivalent variation for six large flare spectra as a function of water slab thickness.

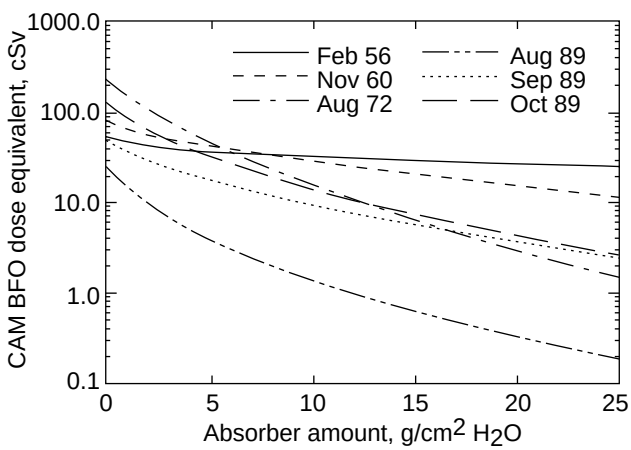

Figure 9. Dose equivalent variation for six large flare spectra evaluated with CAM BFO thickness distribution.

Ordinary Solar Proton Events

A precise definition of a "large proton flare" does not exist. The exact meaning of the term "ordinary" proton event is also somewhat nebulous in the context of space radiation exposure. For the present purposes, such an event is defined as a proton flare that is not in the category of a large flare, but has an integral fluence of at least 10^7 particles/cm^2 for protons with energies greater than 10 MeV. For solar cycle 21 (1975–1986), the fluence spectra of 55 flares in this category were recorded from instrumented satellite platforms (ref. 16). The fluence spectra for each of these ordinary flares are shown in figure 10, where the wide variations in fluences at a given energy and the fluence-energy gradients are obvious. The total proton fluence spectrum for the entire cycle is also shown. Again the $1/R^2$ dependence of fluence will be assumed for locations other than 1 AU. The Langley nucleon transport code BRYNTRN has been implemented to compute dose-versus-depth functions for the 55 ordinary flares (ref. 17) and for the total proton fluence spectrum (fig. 11). To simplify the dose calculations, only the slab dose results are included in the data base for the individual 55 flares. However, the detailed CAM calculations are included for the total proton fluence spectrum of the cycle. The flares are assumed to deliver their particle fluence and dose instantaneously. These data are used as a basis for the flare model options described in the following sections.

Statistical flare model. A statistical approach to modeling the occurrence of the ordinary proton events appears more feasible than for the large flares. A cumulative distribution function is derived which represents, as a function of time, the number of flares occurring in the course of a complete solar cycle. The function developed for the current model is based on the cumulative number of flares observed during solar cycle 21 (1975–1986), which is shown (smoothed and normalized) in figure 12. The function indicates that by the third year in the cycle, 12 percent of the flares will have occurred, and by the ninth year 92 percent of the total has been reached. Also, a noticeable decrease in rate of occurrence is seen near midcycle (between years 4.5 and 5.5); this feature has also been observed for previous cycles. In the statistical model option, all the observed flares of solar cycle 21 are assumed to occur during a complete cycle period, but their time of occurrence within this period will be redistributed in accordance with the distribution function. The reordering of the flares within a cycle is accomplished by associating a sequence of 55 random numbers between 0 and 1 with the original flares of solar cycle 21. For example, in a single simulation, if a sequence of random numbers (based on a uniform 0–1 frequency function) happens to begin as 0.6, 0.82, 0.12, ..., then (from fig. 12) the first three flares observed in cycle 21 would occur in the simulated cycle at years 6.6, 8.0, 3.0, respectively. Since each of the flares may be identified with a specific fluence spectrum and associated dose function, the random redistribution procedure automatically

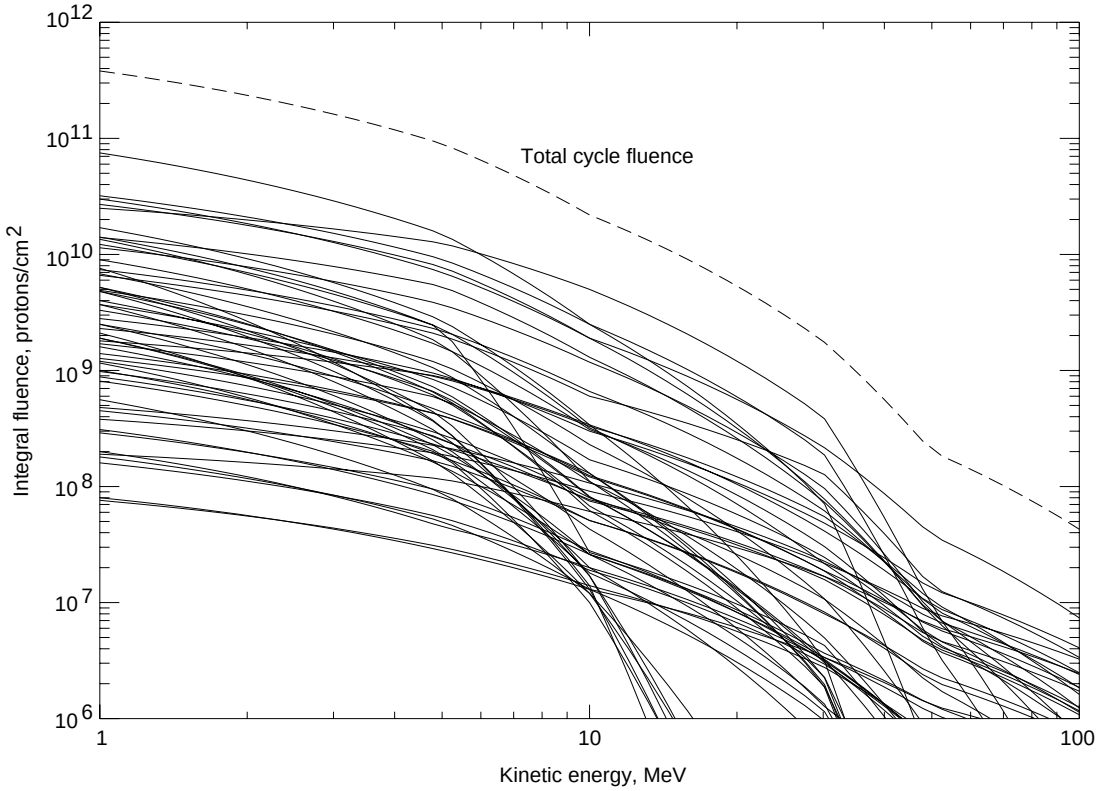

Figure 10. Integral fluence for ordinary proton flares of solar cycle 21.

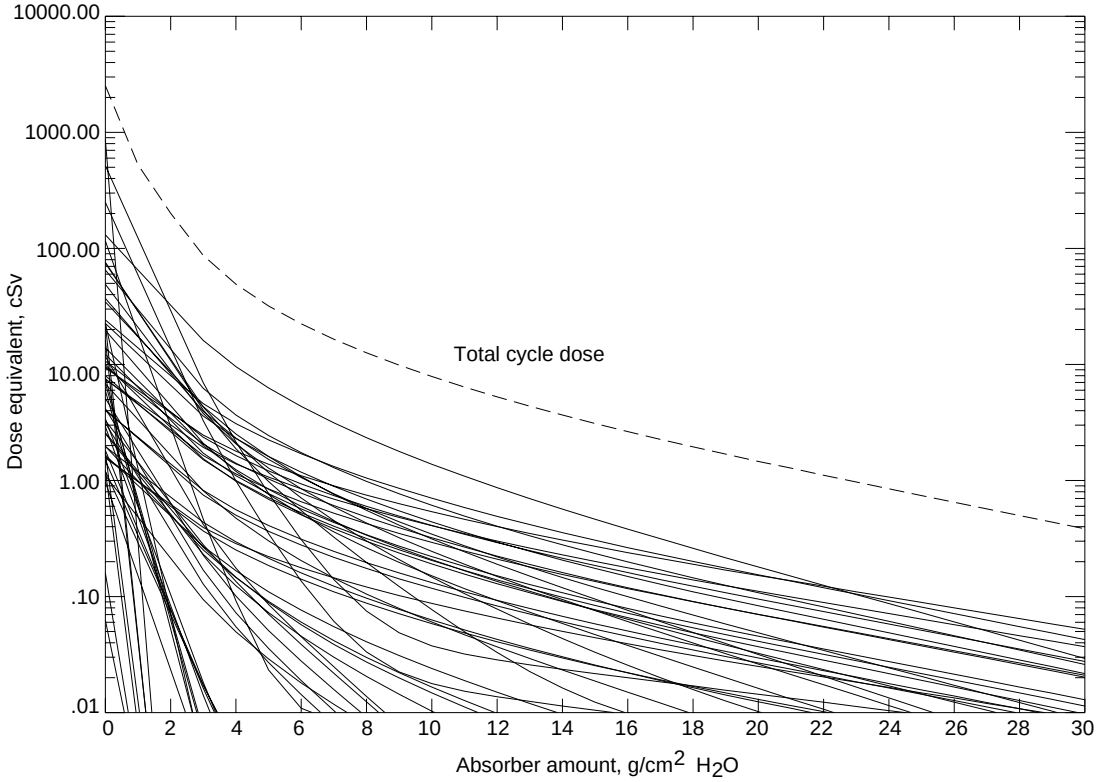

Figure 11. Dose equivalent as a function of water slab amount for ordinary proton flares of solar cycle 21.

leads to a corresponding randomization of particle fluences and dose values over a given mission time. Other statistical approaches have been devised for the flare proton fluences within a solar cycle (refs. 18 and 19) that are not reliant upon only one observed cycle distribution. However, the present scheme does provide reasonable results for mean and deviation of both fluence and dose due to ordinary flares within a given time interval.

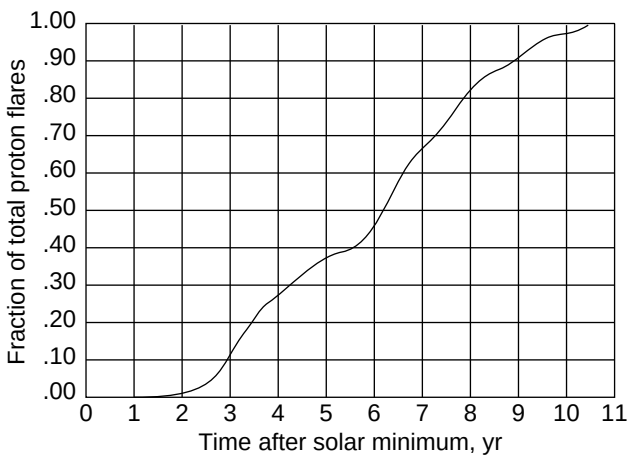

Figure 12. Derived distribution of fractional number of ordinary flares that occur between successive solar minima.

Continuum flare model. The distribution function is also used to define a continuum, or "smeared," model for the ordinary proton flares. In the smeared model, the ordinate of the distribution function is changed from the fraction of total flares having occurred to the fraction of total fluence (or dose) for the cycle, in accordance with the cumulative distribution function. For example, if a conceptual mission takes place between years 5.5 and 7.0 in the solar cycle, the distribution function indicates that 40 percent of the flares have already occurred before the mission, and 67 percent of the flares will have occurred at mission termination. Thus, the portion of the fluence, or corresponding dose, seen during the mission is assumed to be $(0.67 - 0.40)$, or 27 percent of the total cycle value. The continuum model may be used to obtain a single dose or fluence that is representative of a nominal expectation value. If the distribution of values throughout a given range is desired, the statistical model must be used. For parametric mission analyses, the continuum model would normally be preferred for ordinary flare dose contributions; while for a given specific mission scenario, the statistical model may be used to provide uncertainty estimates. Although only slab doses are available in the statistical model, CAM model body geometry effects may be included in the continuum flare model.

Computer Algorithm Structure

The data base for fluences and doses of GCR, large flares, and ordinary flares was developed for use in a computational procedure applicable to missions in interplanetary and cislunar space. The structure of the algorithm is such that implementation both as an independent code and as a subroutine in interplanetary trajectory programs is readily accomplished. Additionally, considerable attention is given to computational efficiency. For example, logic is established that provides options for bypassing portions of the calculation not needed in a given application. A flow diagram of the general computational procedure is given in figure 13.

In the independent, or stand-alone, version of the code, an input file containing the trajectory definition information is required. This file specifies, as a function of solar time, the spacecraft (or target) position in the solar system (in AU) with respect to the Sun. Since the data base is established from environment measurements near the ecliptic plane, use of the model in the general three-dimensional heliosphere would provide results with indeterminate uncertainties. When proximity to planets or moons is a factor (for example, time spent in orbit where planetary shadowing occurs), the target-planet distance is also required, which must be obtained from the detailed trajectory (or orbit) specification. The fractional shadowing factor F_{sh} is computed by MIRACAL as

$$F_{\mathrm{sh}} = 0.5 \left\{ 1 + \cos \left[\sin^{-1} (r_b/r) \right] \right\}$$

where r is the spacecraft distance from the planet center and r_b is the planetary radius. This value corresponds to the fraction of the total solid angle subtended by the planet. This calculation is ignored for $r_b/r < 0.125$, or $F_{\mathrm{sh}} > 0.996$. In the subroutine version, solar and planetary distance variables may be included as needed.

In addition to the data base and trajectory information, an input file is required that establishes the desired options and mission parameters.

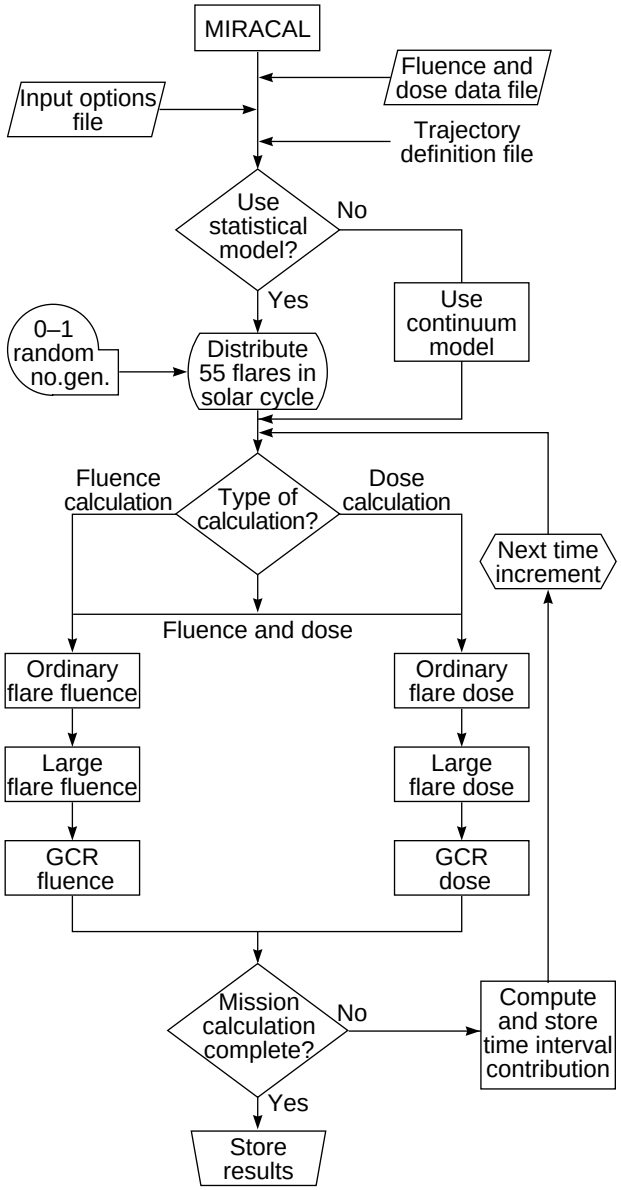

Figure 13. Computational flow diagram for MIRACAL space radiation analysis program.

This setup file enables the user to make a variety of calculations without recompilation of the source code. The user-specified options available are

Input options file:

- Type of calculation (fluence, dose, fluence and dose)
- Flare model type (statistical, smeared)
- Number of large flares occurring during mission (0 to 6)
- Large flare spectrum (Feb. 56, Nov. 60, Aug. 72, Aug. 89, Sep. 89, Oct. 89)
- Times of occurrence of large flares (time in solar cycle)
- Operational shield amount (0 to 25 g/cm^2—integer values)
- Storm shelter shield amount (0 to 25 g/cm^2—integer values)
- Percent crew time in storm shelter (daily fraction)

The option for the type of calculation, either fluence and/or dose estimates, allows the user to bypass portions of the code and thereby enhance computational efficiency. For example, mission analyses where relative human risk estimates are investigated would most likely need only the dose calculation. The fluence environment option would ordinarily be used when subsequent, more detailed transport calculations are performed with the generated fluence spectra as input. For example, in shield configuration analysis, the program will provide a reasonable environment spectrum that may be used in a series of transport calculations adapted to the evaluation of specific shield geometries and materials configurations.

The desired solar flare environment is also specified in the input options file. The statistical flare option will require the use of a random number generator that supplies evenly distributed real numbers over the interval of 0 to 1. Many computer operating systems are equipped with such a feature either in a mathematical function library or as an intrinsic function. For each mission calculation using the statistical model, 55 random numbers are supplied and used as ordinate values on the flare distribution function (fig. 12). In this manner, the individual flares of solar cycle 21 are redistributed over the 11-year cycle period. Selection of the smeared flare model will estimate the fluence and doses by using the "total cycle" curves in figures 10 and 11, with the estimates related directly to the mission duration. Additionally, the user will also specify if and when any of the six large solar proton events will occur.

The user may also designate the approximate effective shield thickness of the anticipated transfer vehicle. The thicknesses are specified in integer values between 0 and 25 g/cm^2 of equivalent water for both the daily crew operational area and the storm shelter. Note that the 25-g/cm^2 thickness requires transport data for 30 g/cm^2 in order to evaluate the 5-cm-depth dose for slab BFO calculations. Previous results utilizing the harsh environment of annual solar minimum GCR fluxes in combination with one large flare (Aug. 1972), indicate that shielding equivalent to approximately 20 g/cm^2 of water would be

required to maintain annual 5-cm-depth dose equivalents to 50 cSv (ref. 20). The thickness selected for the storm shelter is assumed to be the total protection provided whether the shelter is assumed to be internal or external to the operational area. The user must also decide what percentage of the crew's time will be spent in the storm shelter each day for increased protection against galactic cosmic radiation. In the event a large or ordinary flare occurs, the crew is automatically assumed to spend the duration of the event in the storm shelter.

Fluence and/or dose data are computed at specified times during a particular mission scenario. The time-dependent dose data are then written to a data file for postprocessing analysis. The final total mission results may be included in the printed output as cumulative fluences along with the corresponding dose equivalent values for 0- and 5-cm-depth slab shields and the CAM model doses for skin, eye, and blood-forming organs. Execution run times for typical calculations are very fast, requiring at most several seconds for an entire trajectory case.

Sample Results

A representative manned Mars mission scenario is used to illustrate the application of the code in which mission total particle fluences and incurred cumulative doses are predicted. This hypothetical mission is similar to several recently proposed (ref. 21) in which the spacecraft proceeds from Earth to Mars, has a brief stay in the vicinity of the planet, and returns to Earth along a route that includes a Venus swing-by. Specific mission trajectory details are shown in figure 14. The starting date for the mission is February 5, 2014. The mission lasts 500 days and includes a 30-day stay at Mars. With respect to the solar cycle, the mission commences at year 6.23 and terminates at year 7.59 after the last solar minimum. Since this mission occurs during active Sun conditions, two large flares are selected to occur: the relatively energetic spectrum of Nov. 1960 and the relatively high flux spectrum of Aug. 1989 (numbers 2 and 4, respectively, in fig. 7). The times of occurrence of these flares are prespecified, with flare number 2 occurring when the spacecraft is in the vicinity of Venus, and number 4 taking place near the time of minimum distance from the Sun, as indicated in figure 14.

First, with the statistical flare model for this case, the dose and fluence statistics are generated for 500 different distributions of ordinary flares. To investigate the differences in the dose and fluence contributions for each of the random distributions, a shielded compartment of 4 g/cm^2 is selected. No storm shelter is assumed. The resultant histograms, or frequency functions, of the 0- and 5-cm tissue slab doses are given in figure 15. The distributions exhibit considerable skewness, with substantial variance about nominal mean values. The single result for the same shielding condition with the smeared flare option is also indicated and seen to correspond more to a mean or median value, rather than the peak value of the distribution.

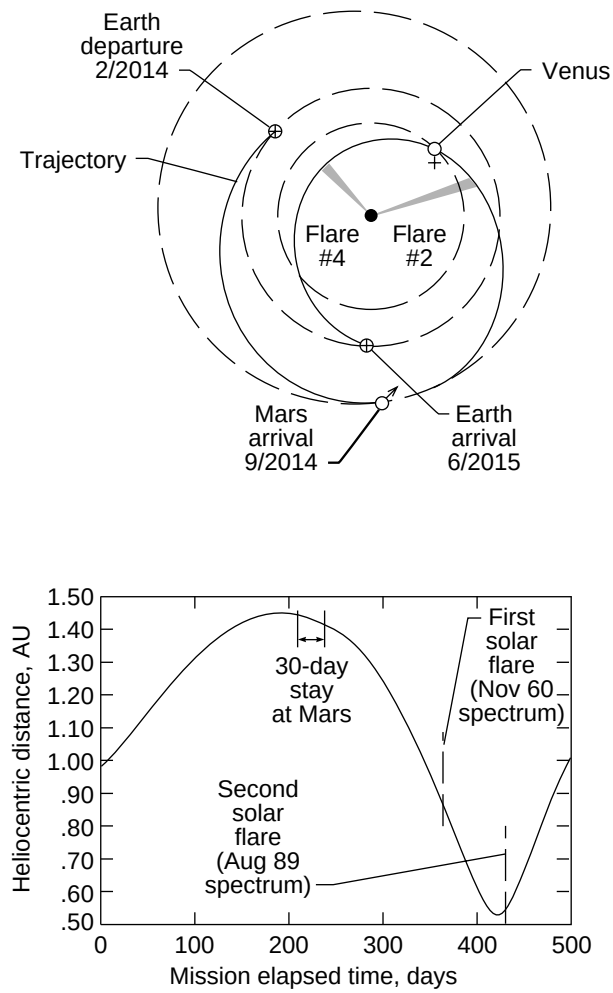

Figure 14. Details of trajectories for manned Mars mission chosen for radiation exposure analysis.

The smeared flare, or "average," dose values of 22 rem and 3.2 rem for the 0- and 5-cm depths, respectively, indicate that 4 g/cm^2 is probably a sufficient shield for the ordinary flare contribution. However, this is not the case for the large flares. Several studies have indicated that heavily shielded compartments will be required (refs. 20 and 22). In addition,

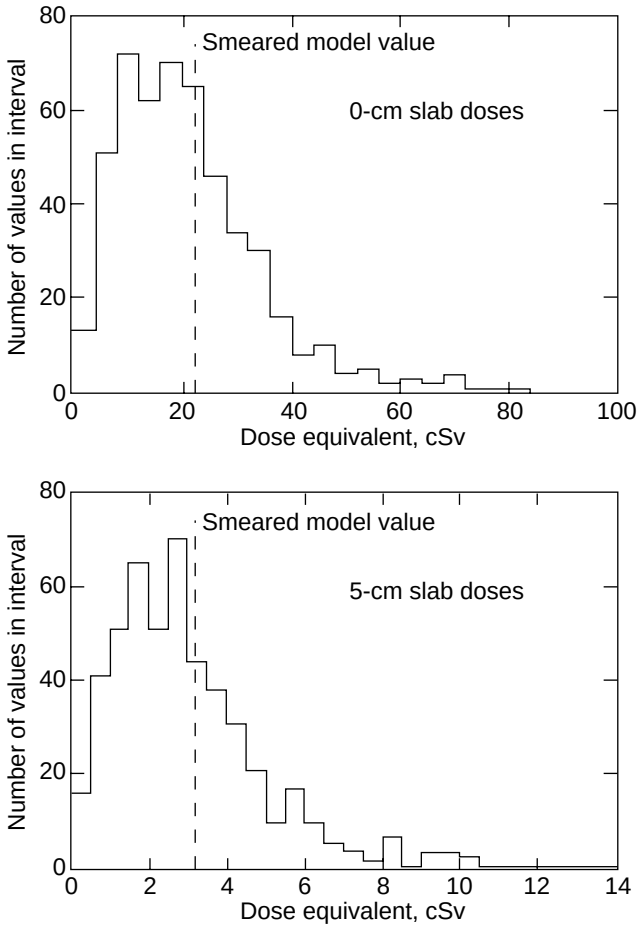

Figure 15. Dose histograms for ordinary flare statistical model. Distributions are for 500 sample cases with 4-g/cm^2 shield.

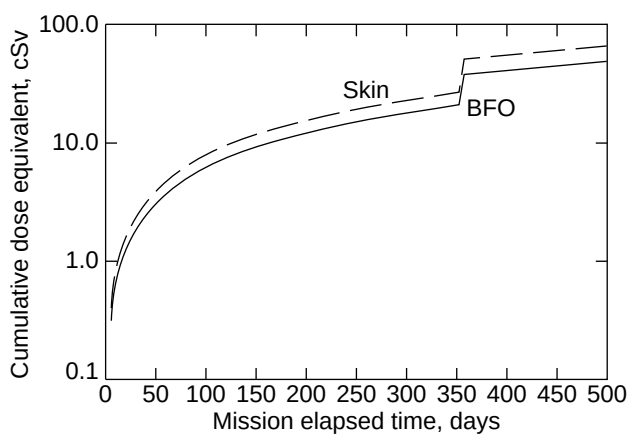

Figure 16. Cumulative dose equivalent for 500-day Mars mission for CAM model skin and BFO calculations.

the GCR component will supply a continuous contribution to the incurred dose. Therefore, for the same scenario, shield thicknesses are next evaluated with a 15-g/cm^2 storm shelter and a 2-g/cm^2 operational area shield. The crew is assumed to remain in the heavily sheltered area during all flare activity and to routinely spend 8 hours per day (33 percent) in the shelter. For these shielding specifications, figure 16 shows the incurred cumulative dose equivalents as a function of mission elapsed time for dose to the skin and blood-forming organs as specified by the CAM body distributions. The corresponding dose to the ocular lens is almost the same as the skin dose and is not shown in the plot. A planetary shadowing factor of 0.7 is used during the Mars stay but is not included at Venus since the trajectory only specified proximity to Venus for a relatively short time (approximately 1 day). The mission total cumulative dose results at the end of the 500-day excursion are given in table II.

Table II. 500-Day Mission Cumulative Dose Equivalents

	Slab doses, cSv		CAM doses, cSv		
	0 cm	5 cm	Skin	Eye	BFO
Ordinary flares	0.94	0.43	0.55	0.55	0.23
Large flares	68.39	43.38	47.02	47.54	29.33
GCR	50.18	38.52	39.97	40.28	31.45
Total	119.51	82.33	87.54	88.37	61.01

For the Mars mission used in the present analysis, table II indicates that the predicted BFO dose may approach or exceed the guideline limits of table I for both annual and 30-day values. Consequently, the time-dependent dosimetric output of the program is examined for 30-day and 1-year cumulative exposures. The resultant skin and BFO dose equivalents are shown in figure 17. For the short term exposure, a rather steady BFO dose equivalent rate of about 2 cSv per 30 days exists for most of the mission, with a slight decrease at mission day 210 when the 1-month stay at Mars begins. During this time a planetary shadowing factor of 0.7 is imposed. At mission day 365, the first of the prescribed flares occurs (Nov. 1960 spectrum) and the BFO dose increases to approximately 30 cSv. The second large flare (Aug. 1989 spectrum) at day 430 is not nearly as severe, with an added BFO dose of only 2 cSv over the GCR background level. The annual cumulative skin and BFO doses are also shown with a practically linear increase for the first year of the mission. If not for the imposed flare occurrence at mission day 365, the annual BFO dose would become essentially constant at approximately 20 cSv/year. However, the flare occurrence superimposes an additional 30 cSv, and with the smaller increase provided by the second

flare, the final mission annual BFO dose exceeds the guideline annual limit of 50 cSv.

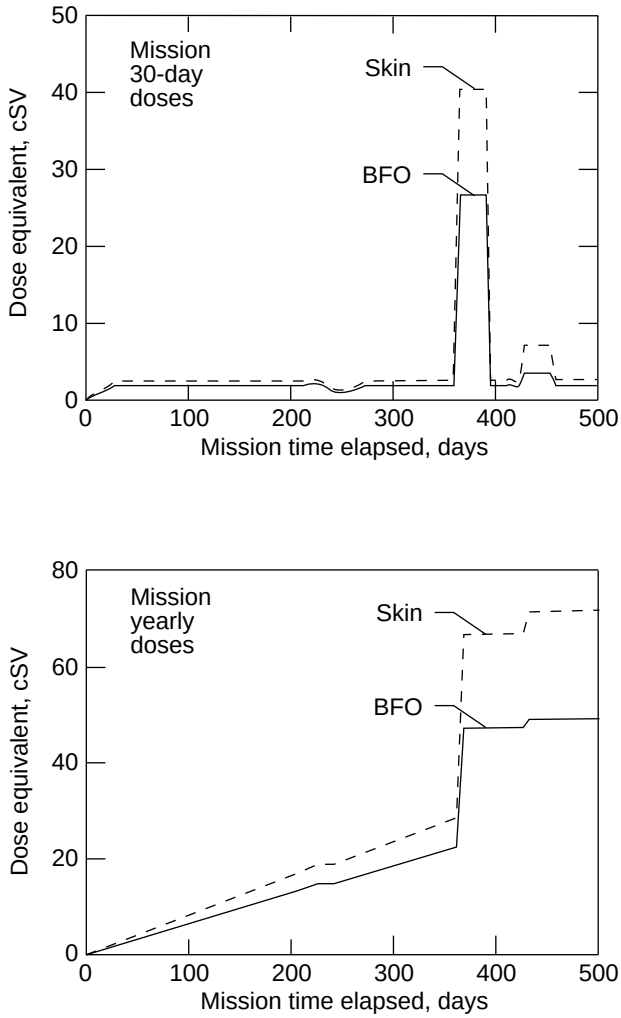

Figure 17. Model results for CAM skin and BFO dose equivalents for cumulative 30-day and annual exposures for the 500-day Mars mission.

The mission total fluence, or cumulative flux, spectra for this mission scenario are given in figure 18 for the ordinary and large flares, and for the five groupings of the GCR nuclei. These data would be applicable as inputs for more detailed transport or shielding calculations that may take into account specific spacecraft and/or shield geometries. In addition, beyond human exposure estimates, such inputs are useful in estimates of degradation and likelihood for failure of optical and electronic components.

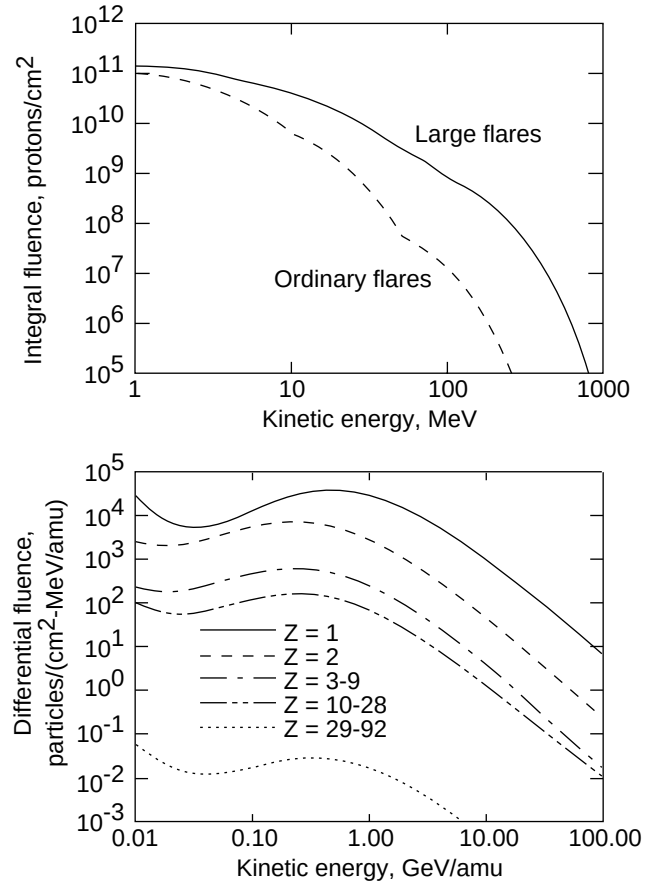

Figure 18. Model results for 500-day Mars mission cumulative particle fluence for deep-space radiations.

Concluding Remarks

The interplanetary environment data base and associated computational procedure for advanced mission radiation exposure analysis should be of value in mission planning activities for future lunar and interplanetary exploration endeavors. The program is computationally efficient (for present mainframe computers, such as the VAX-11/785, with less than 10 sec per run) and easily implemented both as a subroutine and as an independent postprocessing procedure. The data base includes a detailed and extensive representation of the interplanetary heavy charged particle environment with regard to species, their energy distributions, and temporal behavior. The dose-versus-depth variations included in the data base have been constructed from detailed calculations utilizing comprehensive transport codes, which have incorporated rather thorough treatment of particle-shield interaction processes. Also included are estimates of incurred dose equivalents for the human body geometry, which are currently used to evaluate risks due to exposure.

A large number of assumptions are invoked in the construction of the code. Many of the assumptions and approximations are obvious, and some have been noted in the previous descriptions of the data base. Some of the more important assumptions and/or limitations that deserve particular attention are

1. All the solar flares that occur at a given time deliver their associated particle fluences and doses instantaneously.
2. The shield effectiveness (attenuation) data are included only for water and apply only approximately to similar low-density, high-hydrogen-content materials with shield amounts restricted to 25 g/cm^2 or less.
3. An implied assumption of isotropic radiation fields is inherent in the procedure.
4. No specific spacecraft geometries are included; the slab doses apply approximately to the dose at the center of a uniformly shielded spherical shell, and the CAM model body doses are representative of the dose to a human figure at the center of a shielded sphere.
5. Incurred doses from geomagnetically trapped radiations and man-made sources are not included; these may constitute additional important contributions for some missions.

The currently accepted method of evaluating incurred dose equivalents, which is based on energy deposition and relative biological effectiveness parameters, is presently being seriously questioned as to validity in estimating actual risk from exposure to high-energy heavy ions. Present quality factors are based largely on biological experiments involving high-dose-rate exposures of gamma rays and nucleons. Whether the use of these quality factors in extrapolation to the high-energy, low-flux, heavy ion exposures encountered in deep space is conservative with regard to risk is currently unknown. Changes in radiological dosimetric techniques will ultimately require modification of the dosimetric quantities in the present data base. The interplanetary environment model, though based on the best available and most recent data, is also expected to undergo future amendment and enhancement. As the present solar cycle 22 approaches termination in 1996–1997, much additional data will become available for improved modeling of the environment.

Finally, the current code is not formulated for shield design applications, but for use as a method of indicating the relative importance of radiation exposures during various mission scenarios using only tentative estimates of shield requirements. Also, as with any mission radiation analysis, the program has a somewhat limited use in decisions regarding the absolute radiation hazard for a given mission. For example, mission planners are presently not able to accurately prescribe which large flare environment is most reasonable to estimate protection requirements. However, this code should be of considerable value in general mission analysis applications, particularly in mission selection exercises for which radiation exposure is expected to be an important factor.

NASA Langley Research Center
Hampton, VA 23665-5225
April 23, 1992

References

1. National Council on Radiation Protection and Measurements: *Guidance on Radiation Received in Space Activities.* NCRP Rep. No. 98, July 31, 1989.
2. Wilson, John W.; Townsend, Lawrence W.; Nealy, John E.; Chun, Sang Y.; Hong, B. S.; Buck, Warren W.; Lamkin, S. L.; Ganapol, Barry D.; Khan, Ferdous; and Cucinotta, Francis A.: *BRYNTRN: A Baryon Transport Model.* NASA TP-2887, 1989.
3. Townsend, Lawrence W.; Nealy, John E.; Wilson, John W.; and Simonsen, Lisa C.: *Estimates of Galactic Cosmic Ray Shielding Requirements During Solar Minimum.* NASA TM-4167, 1990.
4. Wilson, John W.; Townsend, Lawrence W.; Schimmerling, Walter; Khandelwal, Govind S.; Khan, Ferdous; Nealy, John E.; Cucinotta, Francis A.; Simonsen, Lisa C.; Shinn, Judy L.; and Norbury, John W.: *Transport Methods and Interactions for Space Radiations.* NASA RP-1257, 1991.
5. Adams, J. H., Jr.; Silberberg, R.; and Tsao, C. H.: *Cosmic Ray Effects on Microelectronics. Part I—The Near-Earth Particle Environment.* NRL Memo. Rep. 4506–Pt. I, U.S. Navy, Aug. 1981. (Available from DTIC as AD A103 897.)
6. *Interplanetary Charged Particles.* NASA Space Vehicle Design Criteria (Environment). NASA SP-8118, 1975.
7. Nealy, John E.; Simonsen, Lisa C.; Wilson, John W.; Townsend, Lawrence W.; Qualls, Garry D.; Schnitzler, Bruce G.; and Gates, Michelle M.: Radiation Exposure and Dose Estimates for a Nuclear-Powered Manned Mars Sprint Mission. *Proceedings of the Eighth Symposium on Space Nuclear Power Systems,* Part Two, Mohamed S. El-Genk and Mark D. Hoover, eds., CONF-910116, American Inst. of Physics, 1991, pp. 531–536.
8. *Recommendations of the International Commission on Radiological Protection.* ICRP Publ. 26, Pergamon Press, Jan. 17, 1977.

9. Wilson, John W.; Khandelwal, Govind S.; Shinn, Judy L.; Nealy, John E.; Townsend, Lawrence W.; and Cucinotta, Francis A.: *Simplified Model for Solar Cosmic Ray Exposure in Manned Orbital Flights.* NASA TM-4182, 1990.

10. Billings, M. P.; and Yucker, W. R.: *The Computerized Anatomical Man (CAM) Model.* NASA CR-134043, 1973.

11. Withbroe, George L.: Solar Activity Cycle: History and Predictions. *J. Spacecr. & Rockets,* vol. 26, no. 6, Nov.–Dec. 1989, pp. 394–402.

12. Townsend, Lawrence W.; Wilson, John W.; and Nealy, John E.: *Preliminary Estimates of Galactic Cosmic Ray Shielding Requirements for Manned Interplanetary Missions.* NASA TM-101516, 1988.

13. Nealy, John E.; Wilson, John W.; and Townsend, Lawrence W.: *Solar-Flare Shielding With Regolith at a Lunar-Base Site.* NASA TP-2869, 1988.

14. Simonsen, Lisa C.; Nealy, John E.; Townsend, Lawrence W.; and Wilson, John W.: *Radiation Exposure for Manned Mars Surface Missions.* NASA TP-2979, 1990.

15. Sauer, Herbert H.; Zwickl, Ronald D.; and Ness, Martha J.: *Summary Data for the Solar Energetic Particle Events of August Through December 1989.* Space Environment Lab., National Oceanic and Atmospheric Adm., Feb. 21, 1990.

16. Goswami, J. N.; McGuire, R. E.; Reedy, R. C.; Lal, D.; and Jha, R.: Solar Flare Protons and Alpha Particles During the Last Three Solar Cycles. *J. Geophys. Res.*, vol. 93, no. A7, July 1, 1988, pp. 7195–7205.

17. Nealy, John E.; Simonsen, Lisa C.; Townsend, Lawrence W.; and Wilson, John W.: *Deep-Space Radiation Exposure Analysis for Solar Cycle XXI (1975–1986).* SAE Tech. Paper Ser. 901347, July 1990.

18. Feynman, Joan; and Gabriel, Stephen B.: A New Model for Calculation and Prediction of Solar Proton Fluences. AIAA-90-0292. Jan. 1990.

19. Stassinopoulos, E. G.: *SOLPRO: A Computer Code To Calculate Probabilistic Energetic Solar Proton Fluences.* NSSDC 75–11, National Space Science Data Center, NASA Goddard Space Flight Center, Apr. 1975.

20. Simonsen, Lisa C.; and Nealy, John E.: *Radiation Protection for Human Missions to the Moon and Mars.* NASA TP-3079, 1991.

21. Braun, Robert D.; Powell, Richard W.; and Hartung, Lin C.: *Effect of Interplanetary Trajectory Options on a Manned Mars Aerobrake Configuration.* NASA TP-3019, 1990.

22. Simonsen, Lisa C.; Nealy, John E.; Sauer, Herbert H.; and Townsend, Lawrence W.: Solar Flare Protection for Manned Lunar Missions: Analysis of the October 1989 Proton Flare Event. SAE Tech. Paper Ser. 911351, July 1991.

Table I. NCRP-98 Dose Equivalent Limit Guidelines

Exposure	Skin	Eye	BFO
30-day	150	100	25
Annual	300	200	50
Career	600	400	[a]100–400

[a]Age and gender dependent.

Table II. 500-Day Mission Cumulative Dose Equivalents

	Slab doses, cSv		CAM doses, cSv		
	0 cm	5 cm	Skin	Eye	BFO
Ordinary flares	0.94	0.43	0.55	0.55	0.23
Large flares	68.39	43.38	47.02	47.54	29.33
GCR	50.18	38.52	39.97	40.28	31.45
	—	—	—	—	—
Total	119.50	82.33	87.54	88.37	61.02